X-621-69-551
PREPRINT

NASA TM X-63877

AN EXPERIMENTAL STUDY OF THE ION CHEMISTRY AND THERMAL BALANCE IN THE E AND F REGIONS ABOVE WALLOPS ISLAND

M. W. PHARO, III
L. R. SCOTT
H. G. MAYR
L. H. BRACE
H. A. TAYLOR, JR.

DECEMBER 1969

GSFC
GODDARD SPACE FLIGHT CENTER
GREENBELT, MARYLAND

X-621-69-551
Preprint

AN EXPERIMENTAL STUDY OF THE ION CHEMISTRY AND THERMAL BALANCE IN THE E AND F REGIONS ABOVE WALLOPS ISLAND

M. W. Pharo, III, L. R. Scott*, H. G. Mayr,

L. H. Brace, and H. A. Taylor, Jr.

Laboratory for Planetary Atmospheres

December 1969

Goddard Space Flight Center

Greenbelt, Maryland

*U. S. Army Element, NASA

AN EXPERIMENTAL STUDY OF THE ION CHEMISTRY AND THERMAL BALANCE IN THE E AND F REGIONS ABOVE WALLOPS ISLAND

INTRODUCTION

Much theoretical and experimental attention has centered on the photochemistry and energy balance of the plasma in the lower thermosphere [Hanson, 1963; Norton et al., 1963; Dalgarno et al., 1963; Holmes et al., 1965; Spencer et al., 1965; Swider, 1965; Donahue, 1966; Bauer, 1966; Johnson et al., 1967; Brace et al., 1969; Brinton et al., 1969]. A shortcoming of most studies is that the investigators considered the problems separately, using ion-composition profiles obtained at one time along with electron concentration and temperature profiles taken at a significantly different time or location, assuming models for unmeasured parameters. Because many photochemical and thermal processes in the atmosphere are interdependent, near-simultaneous measurements are desirable in order to produce a consistency of results when studying the physics of the thermosphere.

This paper presents a set of F region vertical profiles of positive ion composition and electron concentration and temperature obtained above Wallops Island, Virginia, on August 26, 1966. These measurements resulted from experiments flown on Nike-Tomahawk rocket NASA 13.06 at 1351 EST (1851 UT). Measurements of molecular nitrogen concentration and temperature [Spencer et al., 1969]

(Thermosphere Probe NASA 18.05, 1331 EST) and spectroscopic measurements of a few lines in the extreme ultraviolet range [Hinteregger, personal communication] (NASA 4.101, 1313 EST) on the same day just before the NASA 18.06 flight complete the set of data used to study the photochemistry and plasma energy balance simultaneously. This analysis considers the production and loss of ions and electrons in the F-region, as well as the spectrum of ionizing radiation, ionization cross sections, plasma cooling processes, neutral and charged particle concentrations, temperatures, and recombination coefficients. The results include rates of the primary chemical reactions responsible for the formation of the ionosphere as well as those for the electron and ion cooling.

INSTRUMENTATION

The Ion Spectrometer

As the operation of Bennett mass spectrometers has been described by Taylor et al. [1963, 1965], this paper contains only details of this particular experiment. The sensor, a 7-5 cycle cylindrical ceramic tube with 3 mm grid spacing, operated at a frequency of 5.4 MHz. The spectrometer tube was mounted coaxially along with the associated electronics and earth telescope (a part of the optical-aspect system), in one end of the thermosphere probe experiment package. The ion mass range from 12 to 36 amu was scanned every 0.15 seconds.

The Cylindrical Electrostatic Probes

Spencer et al. [1965] have described the derivation of electron temperature (T_e) and concentration (N_e) from electrostatic probe measurements. Two probes made independent measurements on this flight: the probe sensors had identical dimensions (collector: diameter = 0.022 inches, length = 9.0 inches; guard: diameter = 0.067 inches, length = 5.0 inches), but each was made of a different material to permit a study of the electrode surface/plasma interactions upon the measurements. One was made of gold-plated stainless steel; the other was also gold-plated, but made of beryllium copper.

RESULTS

Electrostatic Probe Data

The volt-ampere characteristics from the two probes agreed well throughout the flight. However, the data showed evidence of local contamination, perhaps caused by rocket motor outgassing, during approximately the first 30 seconds after the instrument package was ejected from the nose cone. Consequently, the results below 150 km came from the descent data which did not exhibit this problem. Figures 1 and 2 show the altitude profiles of N_e and T_e respectively. Figure 2 also shows the molecular nitrogen temperature (T_g) profile, derived from the N_2 scale heights measured on NASA 18.05, just 20 minutes earlier, illustrating the difference in T_e and T_g.

Ion Composition

The total ion current detected during each spectral sweep was normalized to a vertical profile of total ion concentration (N_i) to derive the concentrations of the individual ion constituents. This profile was established by assuming $N_i = N_e$ and by normalizing (at F-maximum) the smoothed profile of electron concentration (N_e) measured by the electrostatic probe to a curve resulting from ground based-ionosonde measurements from 130 to 240 kilometers. The electrostatic probe thus provided an extrapolation of the ionosonde profile from F-maximum to peak altitude. Before normalization to the total ion concentration profile, the individual ion-current measurements were corrected for mass discrimination, using factors derived from laboratory data. After the normalization process, we eliminated the wake data; the respective ascent and descent data then agreed within 20 percent. Averaging these remaining points produced the final profiles shown in Figure 1.

DISCUSSION

The Electron and Ion Thermal Balance

By employing the profile of T_e measured by the electrostatic probe experiment on this flight to calculate the electron cooling rates as a function of altitude, the derived electron and ion thermal balance can be compared to earlier results of measurements by Spencer et al. [1965] and Brace et al. [1969]. In the derivation the procedure described by Brace et al. [1969] was used except that

the effects of electron heat conduction (following Banks [1966]) were also included. The ion temperature (T_i) was calculated by equating the electron-ion heating rate to the ion-neutral cooling rate. As mentioned earlier, N_2 temperatures (see Figure 2) and concentrations were obtained from measurements reported by Spencer et al. [1967, 1969]. The Jacchia 1964 model atmosphere provided the remaining neutral constituent concentrations, using the measured neutral temperature to determine the appropriate model. Figure 3 shows the calculated local electron cooling rate (solid line) and the local heating rate (dashed line). The difference indicates the amount of heat conducted into or out of the region, showing that above 210 kilometers heat conduction acts as a heat source, below a heat sink. The net effect is that the F_1 region peak of local cooling shifts to a higher altitude than the peak of local heating. At altitudes below 160 kilometers the rates increase toward higher values, and exhibit maximum values in the E-region. The cooling rates, throughout the entire range of altitude, resemble those derived from data obtained at Wallops Island in 1960 and 1961 [Spencer et al., 1965] at similar levels of solar activity ($F_{10.7}$ = 125 vs $F_{10.7}$ = 103 for the 18.06 flight).

Ion Chemistry

The basis of our photochemical analysis was the ultraviolet spectrum and the absorption and ionization cross sections given by Hinteregger et al. [1965]. The few lines in the EUV spectrum monitored above 300 Å only 40 minutes

before this flight [Hinteregger, personal communication] did not exhibit any consistant trend in intensity variations. However, at the time of the charged particle experiments, the 10.7 cm flux (which reflects the level of solar activity) exceeded by 50 percent its value in 1963 when Hinteregger's measurements were made. Considering that the low wavelengths in the EUV spectrum are especially sensitive to variations in solar activity, we scaled the photon fluxes linearly from a factor of one at 300 Å to a factor of three at 100 Å. This procedure, which keeps the spectral intensities within experimental uncertainties of the earlier EUV measurements, resulted in good agreement with ion composition measurements. We assumed that each 25 ev of photoelectron energy produced one electron/ion pair, giving an efficiency factor of

$$Eff = \frac{E_{ph}}{25}$$

where E_{ph} is the energy of a photon (in ev) for wavelengths smaller than 350 Å; above 350 Å we assumed that the efficiency factor was unity. Figure 4 shows ionization rates for O^+, N_2^+, and O_2^+ (including primary and secondary ionization) calculated by using Jacchia's 1964 model for the unmeasured neutral composition and the measured exospheric temperature (950°K).

N_2^+ Ions

Figure 4 illustrates the production of N_2^+ ions by photoionization of N_2. The loss of N_2^+ ions results primarily from the reactions

$$N_2^+ + O \rightarrow NO^+ + N \qquad \left[k_{N_2^+O}\right] \qquad (1)$$

$$N_2^+ + O_2 \rightarrow O_2^+ + N_2 \qquad \left[k_{N_2^+O_2}\right] \qquad (2)$$

[Ferguson, 1967], and by

$$N_2^+ + e \rightarrow N + N \qquad \left[k_{N_2^+e}\right] \qquad (3)$$

The last reaction is electron-temperature (T_e) dependent, [Biondi, 1967] with

$$k_{N_2^+e} = k_{N_2^+e_0}\left(\frac{300}{T_e}\right)^{0.4}$$

where

$$k_{N_2^+e_0} = 2.5 \times 10^{-7}\ \mathrm{cm^3\ sec^{-1}}$$

Figure 2 shows the T_e altitude distribution. The N_2^+ continuity equation, using the photoproduction rates of N_2^+, the measured concentration of N_e, NO^+, and O_2^+ and reactions 1-3, was solved by varying $k_{N_2^+O}$ and $k_{N_2^+O_2}$ to prcvide an

optimum fit to the observed N_2^+ profiles. The resulting values are

$$k_{N_2^+O} = 8.0 \times 10^{-11} \text{ cm}^3 \text{ sec}^{-1}$$

and

$$k_{N_2^+O_2} = 6.2 \times 10^{-11} \text{ cm}^3 \text{ sec}^{-1} .$$

These values are lower than those summarized by Ferguson [1967] by about a factor of two, which is approximately the uncertainty for the ionization cross sections [Hinteregger, personal communication].

NO^+ Ions

Production of NO^+ ions is by reaction (1) and by reaction

$$O^+ + N_2 \rightarrow NO^+ + N \qquad \left[k_{O^+N_2}\right] \qquad (4)$$

and

$$N^+ + O_2 \rightarrow NO^+ + O \qquad \left[k_{N^+O_2}\right] \qquad (5)$$

[Ferguson, 1967]. Loss of NO^+ is by dissociative recombination

$$NO^+ + e \rightarrow N + O \qquad \left[k_{NO^+e}\right] \qquad (6)$$

with an electron-temperature coefficient of

$$k_{NO^+e} = k_{NO^+e_0} \left(\frac{300}{T_e}\right)^{1.1} \quad (7)$$

where

$$k_{NO^+e_0} = 7 \times 10^{-7} \text{ cm}^3 \text{ sec}^{-1}$$

[Biondi, 1967].

Because the O_2 concentration [Jacchia, 1964] is at least a factor of five lower than the measured N_2 concentration and the measured N^+ concentration is nearly two orders of magnitude lower than the measured O^+ concentration over the entire altitude range (Figure 1), we can neglect reaction (5). With the knowledge of the previously determined coefficient, $k_{N_2^+O}$, we used (1) and (4) and our measurements to evaluate the following coefficient for reaction (4)

$$k_{O^+N_2} = 6.5 \times 10^{-13} \text{ cm}^3 \text{ sec}^{-1} .$$

Laboratory measurements of this coefficient gave an upper limit of 6.7×10^{-12} cm^3 sec^{-1} [Talrose et al., 1962]. Measurements by Fehsenfeld et al [1965b] resulted in a value of 3.0×10^{-12} cm^3 sec^{-1}. Schmeltkopf et al. [1966] reported that this rate may sharply depend on the vibrational temperature of N_2, and this may explain some of the higher values reported for $k_{O^+N_2}$.

O^+ Ions

The O^+ ions are produced by photoionization and by the charge exchange reaction

$$N_2^+ + O \rightarrow O^+ + N_2 \qquad \left[k_{N_2^+O}\right] . \tag{8}$$

Ferguson et al. [1965] estimate the reaction coefficient for (8) to be smaller than 10^{-11} cm^3 sec^{-1}. Considering the N_2^+ density when compared to the O^+ density (Figure 1) that is involved in the subsequent loss reaction, we may neglect (8).

The O^+ ions are removed by reaction (4) and by

$$O^+ + O_2 \rightarrow O_2^+ + O \qquad \left[k_{O^+O_2}\right] \tag{9}$$

[Ferguson, 1967].

Using the production rate for O^+ (Figure 4) and the previously derived rate coefficient, $k_{O^+N_2}$, we found that a coefficient for reaction (9) of

$$k_{O^+O_2} = 5.9 \times 10^{-12} \text{ cm}^3 \text{ sec}^{-1}$$

agrees best with the O^+ measurements. For this rate coefficient the values that occur in the literature vary between 1.8×10^{-12} [Langstroth and Hasted, 1962] and 4×10^{-11} cm^3 sec^{-1} [Fehsenfeld et al., 1965a].

O_2^+ Ions

O_2^+ ions are produced by photoionization (rate shown in Figure 4), by reactions (2) and (9), and (according to Fehsenfeld et al. [1965c]) by

$$N^+ + O_2 \rightarrow O_2^+ + N \qquad \left[k_{N^+O_2}\right]. \tag{10}$$

Removal of O_2^+ is by dissociative recombination

$$O_2^+ + e \rightarrow O_2 \qquad \left[k_{O_2^+e}\right] \tag{11}$$

with

$$k_{O_2^+e} = k_{O_2^+e_0}\left(\frac{300}{T_e}\right)^{0.4}$$

where

$$k_{O_2^+e_0} = 3.0 \times 10^{-7}\ \text{cm}^3\ \text{sec}^{-1}$$

[Biondi, 1967]. Using the reaction rates $k_{O^+O_2}$ and $k_{N_2^+O_2}$ derived earlier, we can estimate the coefficient for $k_{N^+O_2}$, assuming photochemical equilibrium. Our analysis has shown that its value should not be larger than

$$k_{N^+O_2} = 3 \times 10^{-10}\ \text{cm}^3\ \text{sec}^{-1}\ .$$

This is lower than the laboratory values summarized by Ferguson [1967], which vary from 4.5×10^{-10} to 5.0×10^{-10} cm^3 sec^{-1}.

The production mechanisms (2), (9), and (10) and the ionization rate for O_2^+ decrease with altitude, whereas the recombination rate (which is proportional to N_e) tends to increase. From this, although we expected a decrease of O_2^+ above 130 km, we found an essentially constant O_2^+ concentration below 160 km. A possible explanation is that the photoionization rate for O_2^+ is actually lower than we calculated. Then the total production rate would decrease significantly at lower altitudes where the other production mechanisms involving O^+, N^+, and N_2^+ (which decrease with altitude) become less significant.

In order to check the consistency of the derived reaction-rate coefficients we solved the coupled continuity equations for O^+, N_2^+, NO^+, and O_2^+ and the previously discussed ion chemistry reactions for the ion altitude distributions assuming photochemical equilibrium and using the derived reaction rate coefficients. The measured ion profiles diverged from the calculated distributions above 230 km, indicating that diffusion processes are important above this altitude. We did not calculate the N^+ because this procedure involves the He^+ concentration, which was not measured in this experiment. However, the measured N^+ was used where applicable.

Figure 5 shows good agreement between measured and calculated ion distributions below 230 km. The only significant exception is O_2^+ at lower altitudes, which probably indicates that the photoionization cross sections adopted for O_2^+ were too high.

Distributions of NO^+ and O_2^+

Figure 5 shows the measured distributions of NO^+ and O_2^+ to be nearly parallel; in near agreement with the calculated model. These measurements confirm, to an altitude of 240 km, the observation of Holmes et al. [1965] that when NO^+ and O_2^+ are in chemical equilibrium, the scale heights correspond to the scale heights of N_2 and O_2 respectively. Above 240 km a sharp increase in the NO^+ and O_2^+ scale heights is evident. This increase is considered too great to be consistent with the rise in gas temperature in this region. Brinton et al. [1969], suggested that diffusion (and consequently plasma temperatures and polarization fields) governs ion distributions at higher altitudes. It is important to consider the effects of the variability of the neutral composition, the plasma temperatures, and the UV spectrum of the sun upon the ion composition. To investigate this we compared the characteristic times for diffusion and the chemical reactions involving these ion species. The diffusion time is

$$\tau = \frac{H^2}{D} \sim 10^{-7} N \tag{12}$$

where H is the scale height of NO^+ or O_2^+, and the diffusion coefficient, D, is given by

$$D = \frac{kT}{\theta N} \tag{13}$$

where θ is the drag coefficient ($\sim 10^{-33}$ cgs), and N is the total atmospheric density. The production time for NO^+ is

$$\tau = \frac{[NO^+]}{k_{O^+N_2}\,[O^+]\;[N_2]} \sim 7 \times 10^1\,(\text{sec})\,, \tag{14}$$

and the recombination time is

$$\tau = \frac{1}{k_{NO^+e}\,N_e} \sim 3 \times 10^1\,(\text{sec})\,. \tag{15}$$

The altitude where diffusion and chemical reactions are comparable is about 270 km where $N = 7 \times 10^8\ (cm^{-3})$. Above this height diffusion should dominate the NO^+ distribution.

In diffusive equilibrium, assuming for simplicity that T_e is constant with height, the diffusion equation for NO^+ is

$$\frac{1}{[NO^+]}\,\frac{\partial [NO^+]}{\partial z} = -\frac{m_{NO^+}\rho}{k\,T_i} - \frac{T_e}{T_i}\,\frac{1}{N_e}\,\frac{\partial N_e}{\partial z} \tag{16}$$

where m_{NO^+} is the mass of NO^+, and T_i is the ion temperature. From (12) it follows that in the region where diffusive equilibrium prevails (above the F_2 peak) the scale height will increase because of the polarization field (second term in 16). Hence the observed change in the NO^+ scale height and the O_2^+

scale height using similar arguments seems reasonably well understood in terms of the transition from chemical to diffusive processes.

ACKNOWLEDGMENTS

The authors wish to acknowledge their indebtedness to the following individuals and their coworkers at Goddard Space Flight Center, University of Michigan, and Aero Geo Astro, whose participation in the design, development, and calibration of the experiments ensured a successful mission: J. S. Burcham, G. R. Carignan, J. A. Findlay, L. T. Fry, J. R. James, J. Maurer, P. K. Monaghan, D. E. Simons, and Dr. T. C. G. Wagner.

REFERENCES

Banks, P. M., Charged particle temperatures and electron thermal conductivity in the upper atmosphere, Ann. Geophys., 22, 577, 1966.

Bauer, S. J., Chemical processes involving helium ions and the behavior of atomic nitrogen ions in the upper atmosphere, J. Geophys. Res., 71, 1508, 1966.

Biondi, M. A., Recombination processes (charged particles), DASA Reaction Handbook, DASA Information and Analysis Center, Santa Barbara, Cal., DASA 1948, Ch. 11, 1967.

Brace, L. H., H. G. Mayr, and G. R. Carignan, Measurements of electron cooling rates in the midlatitude and auroral-zone thermosphere, J. Geophys. Res., 74, 257, 1969.

Brinton, H. C., M. W. Pharo, III, H. G. Mayr, and H. A. Taylor, Jr., Implications for ionospheric chemistry and dynamics of a direct measurement of ion composition in the F_2 -region, J. Geophys. Res., 74, 2941, 1969.

Dalgarno, A., M. B. McElroy, and R. J. Moffett, Electron temperature in the ionosphere, Planet. Space Sci., 11, 463, 1963.

Donahue, T. M., On the ionospheric conditions in the D region and lower E region, J. Geophys. Res., 71, 1966.

Fehsenfeld, F. C., P. D. Goldan, A. L. Schmeltekopf, and E. E. Ferguson, Laboratory measurement of the rate of the reaction $O^+ + O_2 \rightarrow O_2^+ + O$ at thermal energy, Planet. Space Sci., 13, 579, 1965a.

Fehsenfeld, F. C., A. L. Schmeltekopf, and E. E. Ferguson, Some measured rates for oxygen and nitrogen ion-molecule reactions of atmospheric importance, including $O^+ + N_2 \rightarrow NO + N$, Planet. Space Sci., 13, 219, 1965b.

Fehsenfeld, F. C., A. L. Schmeltekopf, and E. E. Ferguson, Correction in the laboratory measurement of the rate constant for $N_2^+ + O_2 \rightarrow N_2 + O_2^+$ at 300°K, Planet. Space Sci., 13, 919, 1965c.

Ferguson, E. E., Ionospheric ion-molecule reaction rates, Rev. Geophys., 5, 305, 1967.

Ferguson, E. E., F. C. Fehsenfeld, P. D. Goldan, A. L. Schmeltekopf, and M. I. Schiff, Laboratory measurement of the rate of the reaction $N_2^+ + O \rightarrow NO^+ + N$ at thermal energy, Planet. Space Sci., 13, 823, 1965.

Hanson, W. B., Electron temperatures in the upper atmosphere, Space Research 3, 282, 1963.

Hinteregger, H. E., L. A. Hall, and G. Schmidtke, Solar XUV radiation and neutral particle distribution in July 1963 thermosphere, Space Research 5, 1175, 1965.

Holmes, J. C., C. Y. Johnson, and J. M. Young, Ionospheric chemistry, Space Research 5, 756, 1965.

Jacchia, L. G., Static diffusion models of the upper atmosphere with empirical temperature profiles, Smithsonian Institution Astrophysical Observatory, Special Rept. 170, Cambridge, Mass., December 1964.

Johnson, C. Y., Ion and neutral composition of the ionosphere, paper presented at IQSY/COSPAR Joint Symposium, London, United Kingdon, July 1967.

Langstroth, G. F. O., and J. B. Hasted, Disc. Faraday Soc., 33, 298, 1962.

Norton, R. B., T. E. Van Zandt, and J. S. Denison, A model of the atmosphere and ionosphere in the E and F_1 regions, Proceedings of the International Conference on the Ionosphere, A. C. Strickland, ed., London Institute of Physics and Physical Society, 26, 1963.

Schmeltekopf, A. L., F. C. Fehsenfeld, G. L. Gilman, and E. E. Ferguson, Symposium on the physics and chemistry of the lower atmosphere, JILA, Univ. of Colo., June 1966.

Spencer, N. W., L. H. Brace, G. R. Carignan, D. R. Taeusch, and H. Niemann, Electron and molecular nitrogen temperature and density in the thermosphere, J. Geophys. Res., 70, 2665, 1965.

Spencer, N. W., G. R. Carignan, and D. R. Taeusch, Recent measurements of the lower thermosphere structure, NASA Goddard Space Flight Center Rept. X-623-67-480, Sept. 1967.

Spencer, N. W., G. P. Newton, G. R. Carignan, and D. R. Taeusch, Thermosphere temperature variation with increasing solar activity, paper presented at the 12th Plenary Meeting of COSPAR, Prague, Czechoslovakia, May 1969.

Swider, W., Jr., A study of the nighttime ionosphere and its reaction rates, J. Geophys. Res., 70, 4856, 1965.

Talrose, V. L., M. I. Markin, and I. K. Larin, The reaction $O^+ + N_2 \rightarrow NO^+ + N$, Disc. Faraday Soc., 33, 257, 1962.

Taylor, H. A., Jr., L. H. Brace, H. C. Brinton, and C. R. Smith, Direct measurements of helium and hydrogen ion concentration and total ion density to an altitude of 940 kilometers, J. Geophys. Res., 68, 5339, 1963.

Taylor, H. A., Jr., H. C. Brinton, and C. R. Smith, Positive ion composition in the magnetoionosphere obtained from the OGO-A satellite, J. Geophys. Res., 70, 5769, 1965.

FIGURE CAPTIONS

Figure 1. Altitude profiles of measured electron and ion concentrations. The ion concentrations are an average of ascent and descent data, derived by normalizing the ion currents to the total ion concentration, N_i, which is derived from ground based ionosonde measurements and above 240 kilometers, the electrostatic probe data. Below 150 kilometers only the descent electrostatic probe data are shown.

Figure 2. Altitude profiles of T_e and T_g derived from experimental measurements on NASA 18.06 and NASA 18.05 respectively.

Figure 3. Altitude profiles of derived local electron cooling and heating rates. The difference indicates the heat conduction into or out of the region.

Figure 4. Calculated photoproduction rates for O_2^+, N_2^+, and O^+.

Figure 5. Comparison of altitude profiles of ion concentrations calculated assuming photochemical equilibrium and derived reaction rates with the ion concentrations measured by the ion spectrometer on NASA 18.06.

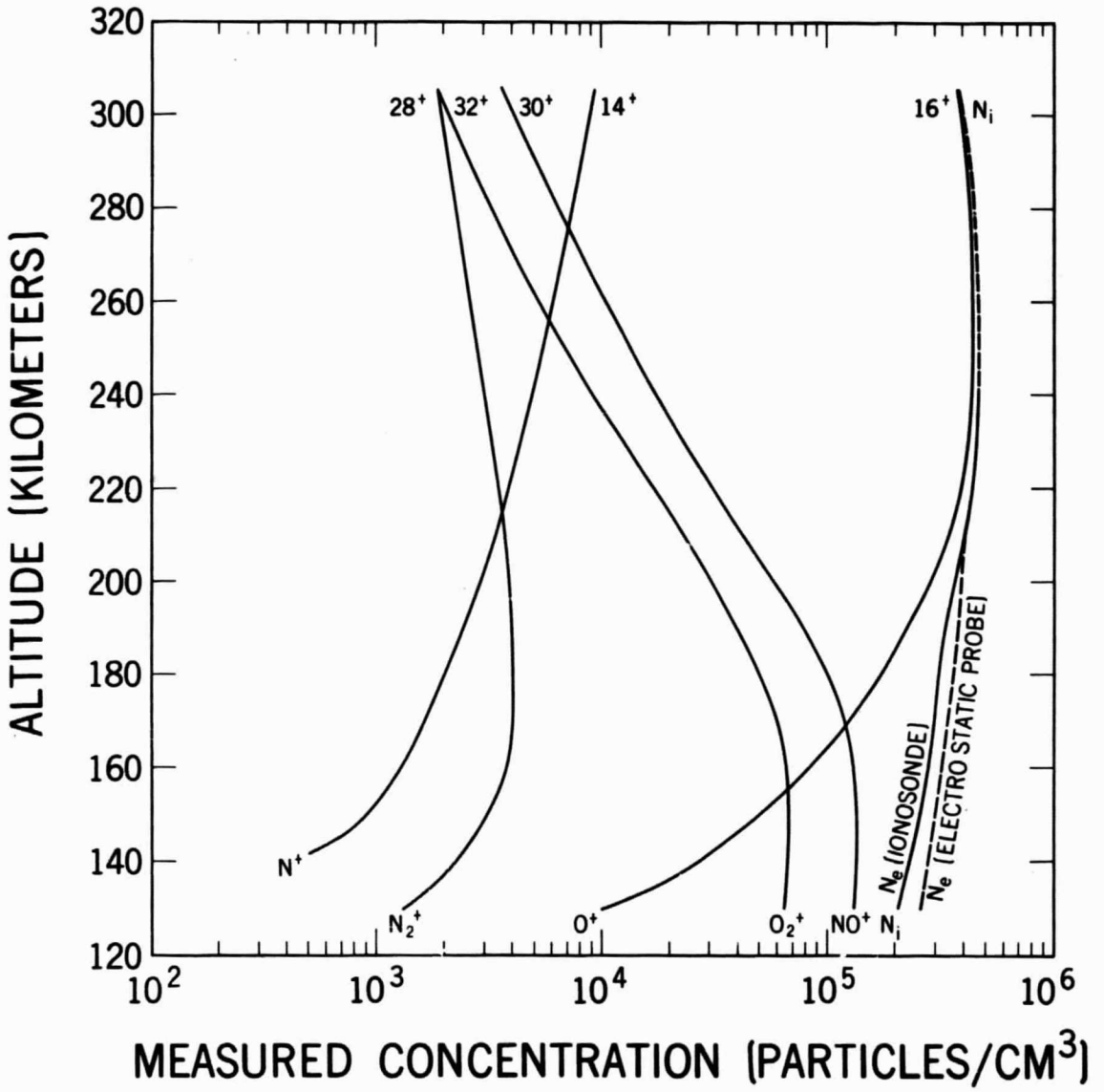

Figure 1–Altitude profiles of measured electron and ion concentrations. The ion concentrations are an average of ascent and descent data, derived by normalizing the ion currents to the total ion concentration, N_i, which is derived from ground based ionosonde measurements and above 240 kilometers, the electrostatic probe data. Below 150 kilometers only the descent electrostatic probe data are shown.

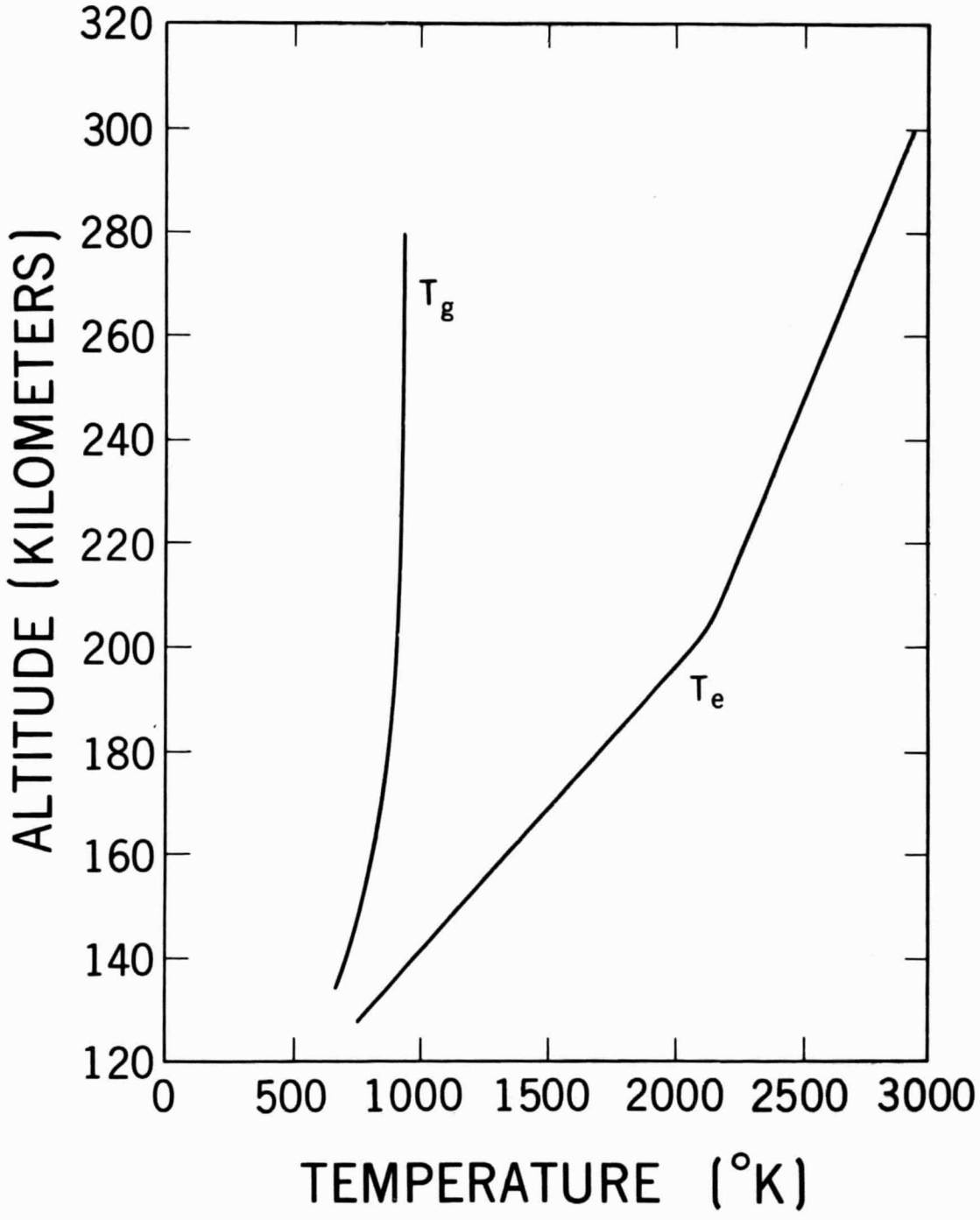

Figure 2–Altitude profiles of T_e and T_g derived from experimental measurements on NASA 18.06 and NASA 18.05 respectively.

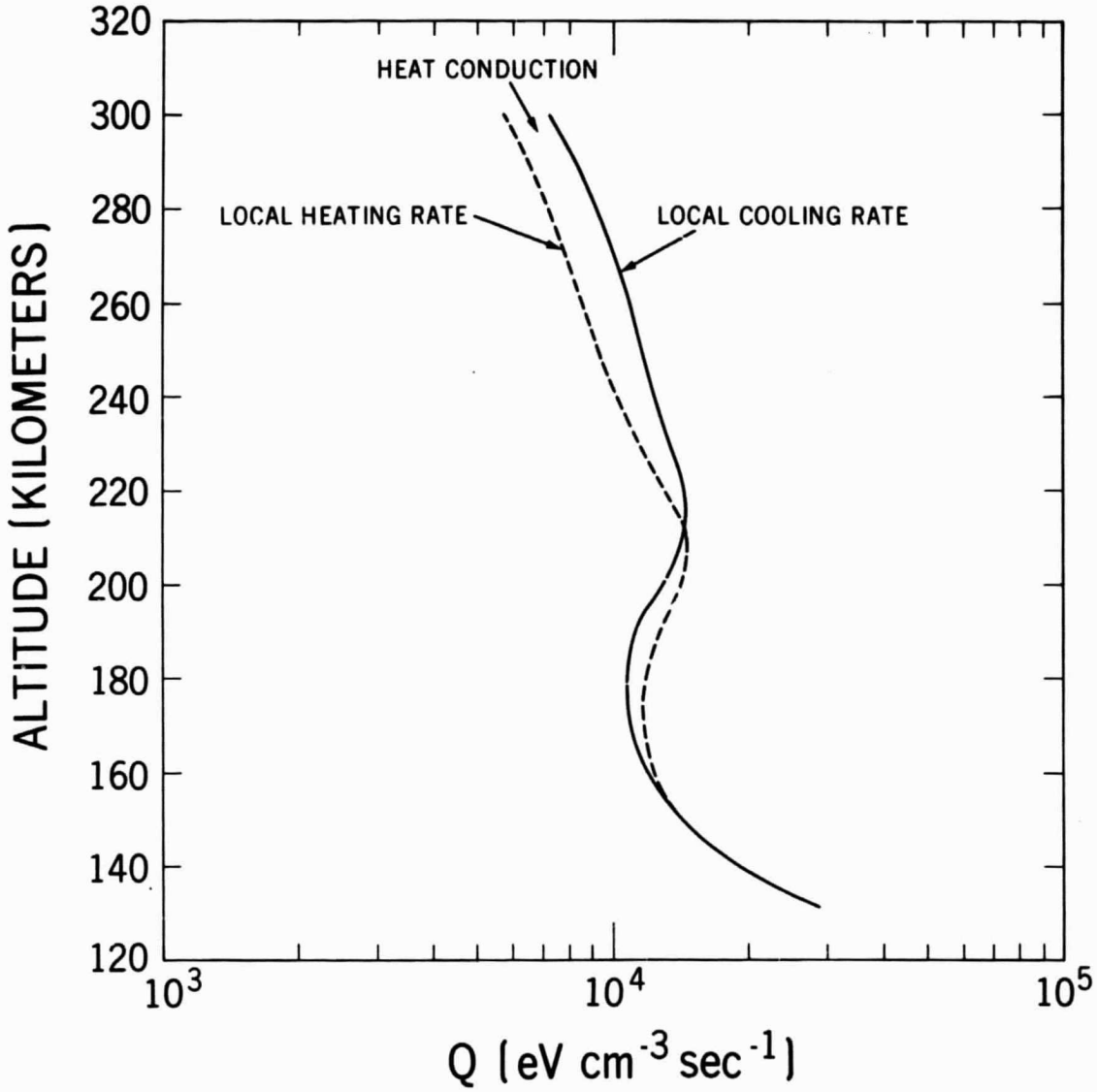

Figure 3–Altitude profiles of derived local electron cooling and heating rates. The difference indicates the heat conduction into or out of the region.

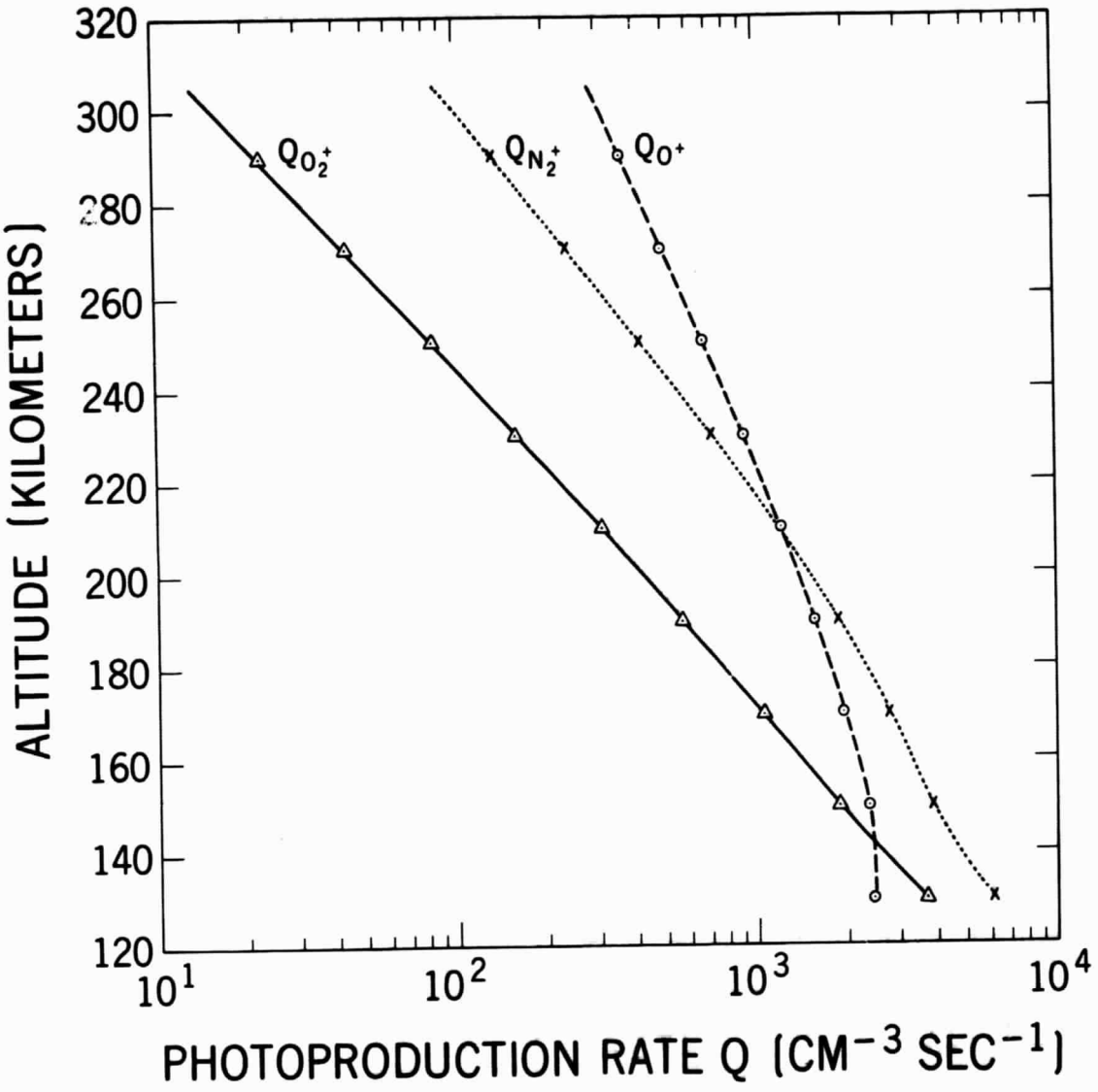

Figure 4–Calculated photoproduction rates for O_2^+, N_2^+ and O^+.

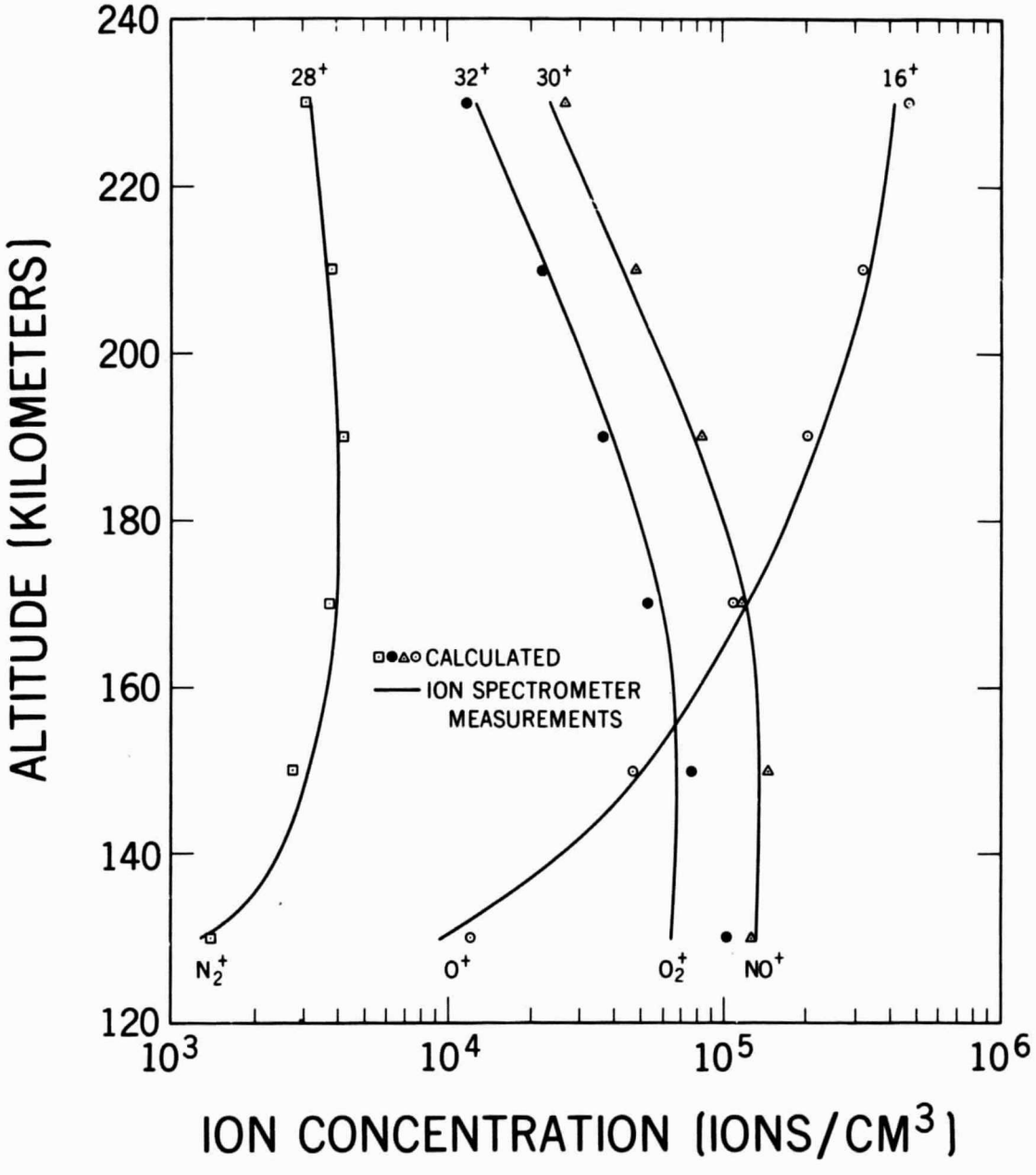

Figure 5–Comparison of altitude profiles of ion concentrations calculated assuming photochemical equilibrium and derived reaction rates with the ion concentrations measured by the spectrometer on NASA 18.06.